



1 SOC sequestration potentials for agricultural management 2 practices under climate change

3 Tobias Herzfeld¹, Jens Heinke¹, Susanne Rolinski¹ and Christoph Müller¹

4 ¹Potsdam Institute for Climate Impact Research, Member of the Leibniz Association, P.O. Box 60 12 03,
5 14412 Potsdam, Germany.

6 *Correspondence:* Tobias Herzfeld (tobias.herzfeld@pik-potsdam.de)

7 **Abstract.** Sequestration of soil organic carbon (SOC) on cropland has been proposed as a climate change
8 mitigation strategy to reduce global greenhouse gas (GHG) concentrations in the atmosphere, which is in
9 particular needed to achieve the targets proposed in the Paris Agreement to limit the increase in atmospheric
10 temperature to well below 2 °C. We here analyze the historical evolution and future development of cropland
11 SOC using the global process-based biophysical model LPJmL, which was recently extended by a detailed
12 representation of tillage practices and residues management (version 5.0–tillage2). We find that model results for
13 historical global estimates for SOC stocks are at the upper end of available literature, with ~2650 Pg C of SOC
14 stored globally in the year 2018, of which ~170 Pg C are stored in cropland soils. In future projections, assuming
15 no further changes in current cropland patterns and under four different management assumptions with two
16 different climate forcings, RCP2.6, and RCP8.5, results suggest that agricultural SOC stocks decline in all
17 scenarios, as the decomposition of SOC outweighs the increase of carbon inputs into the soil from altered
18 management practices. Different climate-change scenarios, as well as assumptions on tillage management, play a
19 minor role in explaining differences in SOC stocks. The choice of tillage practice explains between 0.2% and
20 1.3% of total cropland SOC stock change in the year 2100. Future dynamics in cropland SOC are most strongly
21 controlled by residue management, whether residues are left on the field or harvested. We find that on current
22 cropland, global cropland SOC stocks decline until the end of the century by only 1.0% to 1.4% if residue-
23 retention management systems are generally applied and by 26.7% to 27.3% in case of residues harvest. For
24 different climatic regions, increases in cropland SOC can only be found for tropical dry, warm temperate moist,
25 and warm temperate dry regions in management systems that retain residues.

26 1 Introduction

27 To meet the targets of the Paris Agreement of 2015 to keep the increase in global mean temperature well below
28 2°C, and especially for the ambitious target of below 1.5°C, several negative emission technologies which
29 remove carbon dioxide (CO₂) from the atmosphere have been proposed (Minx et al., 2018; Rogelj et al., 2018,
30 2016). At the same time as the climate is warming, the global human population is expected to increase to 9.7
31 billion people in 2050 and 10.9 billion by 2100 (United Nations et al., 2019), putting additional pressure on
32 future food production systems. Food production alone has to increase by at least 50% (FAO, 2019) or even



33 double by the year 2050, depending on dietary preferences, demographical trends, and climate projections, when
34 global food demand is to be met (Bodirsky et al., 2015). Different agricultural management practices have been
35 proposed as carbon (C) sequestration strategies to mitigate climate change and increase the quality and health of
36 the soil by increasing soil organic carbon (SOC) content of cropland soils (Lal, 2004), which also decreases the
37 risk of soil erosion and soil degradation (Lal, 2009).

38 The potential of SOC sequestration for agricultural management practices, e.g. the effect of no-till, is debated
39 in the scientific community (Baker et al., 2007; Powlson et al., 2014). Minasny et al. (2017) have proposed the ‘4
40 per 1000 Soils for Food Security and Climate’ initiative, which targets to increase global SOC sequestration by
41 0.4% per year. They argue that under best-management practices, this target rate could be even higher. This
42 approach would translate into a 2-3 Pg C a⁻¹ SOC increase in the first 1 m of the soil, which is equivalent to
43 about 20-35% of global greenhouse gas (GHG) emissions (Minasny et al., 2017). This proposal has been
44 criticized, as it overestimates the possible effect of SOC sequestration potential through agricultural management
45 (de Vries, 2018; White et al., 2018). Field trials on SOC sequestration potentials show results with higher, as
46 well as lower sequestration rates, but only represent the local soil and climatic conditions for the time of the
47 experiment (Fuss et al., 2018; Minx et al., 2018), which reduces the likelihood for their validity on larger scales
48 or longer time periods.

49 Global total SOC stocks are estimated between 1500 Pg C (excluding permafrost regions) (Hiederer et al.,
50 2011) to up to 2456 Pg C for the upper 200 cm (Batjes, 2014) and agricultural SOC stocks alone, which are
51 subject to agricultural management, are estimated to be between 140 and 327 Pg C depending on soil depth
52 (Jobbágy and Jackson, 2000; Zomer et al., 2017). Since the beginning of cultivation by humans approximately
53 12000 years ago, global SOC stocks for the top 200 cm of soil have declined by 116 Pg C because of agriculture
54 by one estimate (Sanderman et al., 2017). Management assumptions play an important role in these estimates,
55 e.g. Pugh et al. (2015) found that residue removal and tillage effects contribute to 6% and 8% of total land-use
56 change (LUC) emissions between the year 1850 and 2012 alone, which translates into biomass and soil C losses
57 of approx. 13.5 Pg C and 16 Pg C, respectively.

58 In this study, we use a modeling approach to quantify the historical development of global cropland SOC
59 stocks using new data for agricultural management such as manure and residues management, as well as a new
60 data set of the spatial distribution of tillage practices. In addition, we investigate the potential for SOC
61 sequestration under different climate-change scenarios on current cropland.

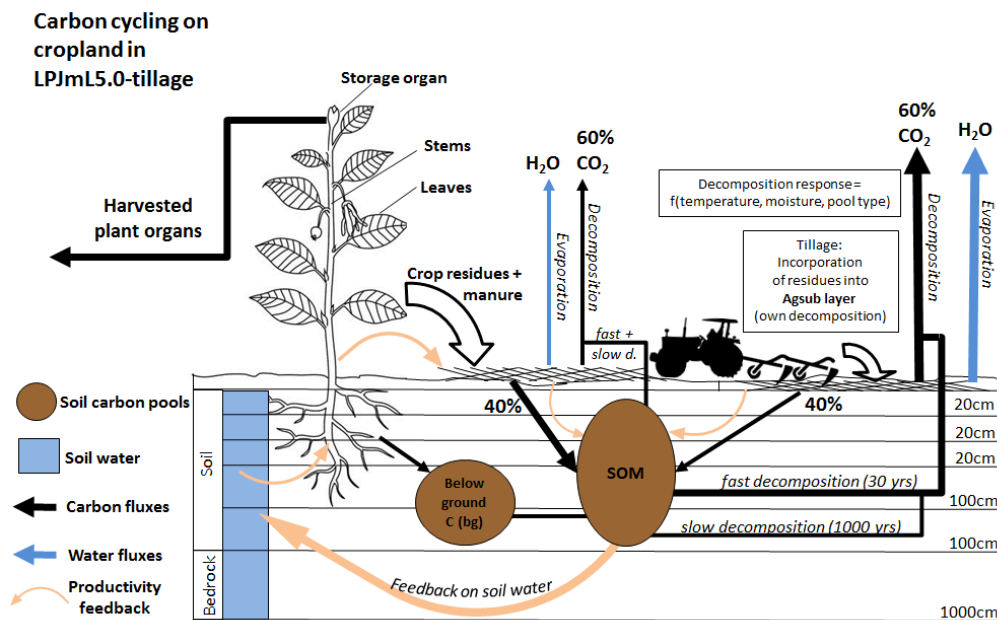
62 **2 Materials and methods**

63 **2.1 The LPJmL5.0-tillage2 model**

64 The LPJmL5.0-tillage2 model combines the dynamic phenology scheme of the natural vegetation (Forkel et al.,
65 2014), with version 5.0-tillage, which covers the terrestrial nitrogen cycle (von Bloh et al., 2018) and the
66 representation of tillage practices and residue management (Lutz et al., 2019b). The model code is available at:
67 <https://doi.org/10.5281/zenodo.4625868> (Herzfeld et al., 2021). All organic matter pools in vegetation, litter, and



68 soil in LPJmL5.0-tillage2 are represented by C pools and the corresponding N pools with variable C:N ratios.
 69 For soil carbon, the slow and fast soil pools are explicitly distributed over five soil layers (Schaphoff et al.,
 70 2013). With the term ‘SOC’ we refer to the sum of all soil and litter C pools. After the harvest of crops, root
 71 carbon is transferred to the below-ground litter pool. The incorporation of above-ground residues into the soil is
 72 dependent on the chosen management practices. Different tillage and residue management schemes and the
 73 accounting for direct effects of SOC on soil hydraulic properties and thus on soil organic matter (SOM)
 74 decomposition and plant productivity have been introduced in the implementation of tillage practices in version
 75 5.0-tillage (Lutz et al., 2019b), and are thus explicitly considered here (Fig. 1).



76

77 **Figure 1: Carbon cycling on cropland and productivity feedbacks from plants to residues and soil stocks and soil**
 78 **water, as modeled in LPJmL5.0-tillage. Arrows indicate fluxes, boxes, and circles are stocks.**

79 In LPJmL5.0-tillage2, the amount of carbon in biomass, which is either harvested or can be left on the field as
 80 crop residue is dependent on productivity (plant growth). Litter pool sizes are determined by the amount of
 81 biomass that is left on the field (i.e. not harvested) and the rate at which the litter is decomposed. At
 82 decomposition, the model assumes a fixed ratio of 40% of C that is transferred from litter to the soil carbon
 83 pools; the other 60% of C are emitted to the atmosphere as CO₂. N cycling is included in the model, explained in
 84 detail in von Bloh et al., (2018), and follows similar principles as SOC decomposition, reflecting the actual C:N
 85 ratios of the decomposing material. Applied N from manure, which is now explicitly considered in contrast to
 86 the previous model version LPJmL5.0-tillage, is assumed to consist of equal shares of mineral and organic N so



87 that 50% is added to the ammonium pool of the first soil layer and the rest is added to the above-ground leaf
88 litter nitrogen pool. The C part of the organic manure is allocated to the leaf litter C pool (i.e. an easily
89 degradable organic pool that can be left on the soil surface or incorporated into the soil column by tillage), with a
90 fixed C:N ratio of 14.5 (IPCC, 2019). Total fertilizer amounts (i.e. mineral fertilizer and manure) are applied
91 either completely at sowing or split into two applications per growing season. Manure is always applied at the
92 first application event at sowing. Only when total combined fertilizer inputs (manure and mineral N) exceed 5
93 gN m⁻², half of the total fertilizer is applied in a second application as mineral fertilizer, which is applied after
94 40% of the necessary phenological heat sums to reach maturity have been accumulated.

95 2.2 Simulation protocol

96 A list of the simulations carried out for this study is summarized in Table 1. An initial spinup simulation per
97 general circulation model (GCM) and Climate Research Unit gridded Time Series (CRU TS) climate data of
98 7000 years is conducted to bring SOC stocks into a dynamic pre-historic equilibrium (SP-GCM/SP-CRU), in
99 which the first 30 years of weather data are cyclically recycled, mimicking stable climate conditions. A second
100 GCM-specific spinup simulation to introduce land use dynamics starts in 1510 so that cropland older than that
101 has reached a new dynamic equilibrium by 1901 when the actual simulations start and land-use history is
102 accounted for otherwise. Simulations were run for three groups: a) historical runs from 1901-2018 using CRU
103 TS Version 4.03 climate input (Harris et al., 2020) and inputs on historical management time series (which is
104 subject to the same spinup procedures as the GCM-specific simulations), b) historical simulations from 1901-
105 2005 with climate inputs from the four GCMs and historical management time series, c) future simulations using
106 projections of the four GCMs for the representative concentration pathways RCP2.6 (low radiative forcing) and
107 RCP8.5 (high radiative forcing) and four different stylized management settings: conventional tillage and
108 residues retained (T_R), conventional tillage and residues removed (T_NR), no-till and residues retained (NT_R)
109 and no-till and residues removed (NT_NR) and d) simulations as in c) but with [CO₂] held constant at the level
110 of the year 2005 (379.8 ppmv) that are used to quantify the CO₂ effect. All other inputs (land-use, N-fertilizer,
111 manure) for all future simulations were also held constant at the year 2005 values. An additional simulation per
112 GCM was conducted where all inputs, as well as management assumptions, are static after 2005. These are used
113 to analyze the business-as-usual case under constant land use (h_cLU). To compare the results to literature
114 values on the maximum potential of global SOC stocks without land use, an additional simulation with potential
115 natural vegetation (PNV) was conducted.



116 **Table 1: Overview of the different simulations conducted for this study. For more details and purposes of the**
 117 **simulation see text. No LU – no land use, PNV – potential natural vegetation.**

| Name | Nr. of sim. | Years | Climate input | Tillage | Residues treatment | Fertilizer | Manure | LU data-set | Description |
|--|-------------|-----------|--|---|--|---|---|---|--|
| SP_CRU SP_GCM | 5 | 7000 | CRU TS 4.03 / HadGEM2_ES, GFDL-ESM2M, IPSL-CM5A-LR, MIROC5 Repeated 1901-1930 | No LU | No LU | No LU | No LU | PNV | 7000 years PNV spin-up until 1509 to compute a pre-historic dynamic SOC equilibrium |
| SPLU_CRU SPLU_GCM | 5 | 390 | CRU TS 4.03 / HadGEM2_ES, GFDL-ESM2M, IPSL-CM5A-LR, MIROC5 Repeated 1901-1930 | First-year values of Porwollik et al. 2019 | First-year values of MADRaT | First-year values of LUH2v2 | First-year values of Zhang et al. (2017) | LUH2v2 (Hurtt et al., 2020) | 390 years spin-up until 1900 to compute the effects of LU history, which is used as the starting point for all simulations |
| h_PNV | 1 | 1901-2018 | CRU TS 4.03 1901-2018 | No LU | No LU | No LU | No LU | PNV | PNV run till 2018 (with 390 years spin-up for better comparability to LU runs), starting from SP_CRU |
| h_dLU | 2 | 1700-2018 | CRU TS 4.03 From 1700-1900 repeated 1901-1930, 1901-2018 afterward | Porwollik et al. 2019 | MADRaT (Dietrich et al., 2020) | LUH2v2 (Hurtt et al., 2020) | Zhang et al. (2017) | LUH2v2 (Hurtt et al., 2020) | Historical run with dynamic LU, starting from SPLU_CRU |
| h_eLU | 2 | 1700-2018 | CRU TS 4.03 From 1700-1900 repeated 1901-1930, 1901-2018 afterward | Porwollik et al. 2019 Static at 2005 level | MADRaT (Dietrich et al., 2020) Static at 2005 level | LUH2v2 (Hurtt et al., 2020) Static at 2005 level | Zhang et al. (2017) Static at 2005 level | LUH2v2 (Hurtt et al., 2020) Static at 2005 level | Historical run with constant land use (with 390 years spin-up as in SPLU_CRU, but with the land use pattern of 2005), starting from SP_CRU |
| h_GCM | 4 | 1901-2005 | HadGEM2_ES, GFDL-ESM2M, IPSL-CM5A-LR, MIROC5 | Porwollik et al. 2019 | MADRaT (Dietrich et al., 2020) | LUH2v2 (Hurtt et al., 2020) | Zhang et al. (2017) | Hurtt 2017 | CMIP5 historical scenario runs use, starting from SPLU_GCM |
| T_R_26/85 NT_R_26/85 T_NR_26/85 NT_NR_26/85 | 64 | 2006-2099 | RCP2.6/RCP8.5 HadGEM2_ES, GFDL-ESM2M, IPSL-CM5A-LR, MIROC5 | tillage / no-till | Residues retained / residues removed | LUH2v2 (Hurtt et al., 2020) Static at 2005 level | Zhang et al. (2017) Static at 2005 level | Hurtt 2017, Static at 2005 level | CMIP5 future runs with different management options, starting from h_GCM |
| TRc05_26 TRc05_85 | 16 | 2006-2099 | RCP2.6/RCP8.5 HadGEM2_ES, GFDL-ESM2M, IPSL-CM5A-LR, MIROC5 | Porwollik et al. 2019 Static at 2005 level | MADRaT (Dietrich et al., 2020) Static at 2005 level | LUH2v2 (Hurtt et al., 2020) Static at 2005 level | Zhang et al. (2017) Static at 2005 level | Hurtt 2017, Constant at 2005 level | CMIP5 future runs with tillage and residue management constant at 2005 level, starting from h_GCM |

118



119 **2.3 Model inputs**

120 We created input data sets for an explicit representation of land use, fertilizer, manure, and residue management,
121 using the MADRaT tool (Dietrich et al., 2020). Historic land-use patterns of shares of physical cropland, also
122 separated into an irrigated and rain-fed area, as well as mineral fertilizer data (application rate per crop in gN m^{-2}
123 a^{-1}) for the period of the year 1900 to 2015, are based on the Land-Use Harmonization – LUH2v2 data (Hurtt et
124 al., 2020), which provides fractional land-use patterns for the period of 850-2015 as part of the Coupled Model
125 Intercomparison Project – CMIP6 (Eyring et al., 2016). Manure application rates for the period 1860-2014 are
126 based on Zhang et al. (2017) and account for organic N. With MADRaT, we were also able to produce data on
127 crop functional type (CFT) specific fractions of residue rates left on the field (recycling shares) for the period
128 1850-2015. We generated data on residue-recycling shares in 5-year time steps for the period 1965-2015 and
129 interpolate linearly between time steps to get an annual time series. Between 1850 and 1965, default recycling
130 shares for cereals of 0.25, for fibrous of 0.3, for non-fibrous of 0.3, and no-use of 0.8 were assigned to 1850 and
131 linearly interpolated to the values of 1965. Cereals include temperate cereals, rice, maize, and tropical cereals;
132 fibrous crops include pulses, soybean, groundnut, rapeseed, and sugarcane; non-fibrous crops include temperate
133 roots, tropical roots, and no-use crops include sunflower, others, pastures, bioenergy grasses and bioenergy trees.
134 Information on conventional tillage and conservation agriculture (no-till) management was based on Porwollik et
135 al. (2019) for the period 1974-2010. Before 1973, conventional tillage was assumed as the default management
136 on all cropland. We assume one tillage event after initial cultivation of natural land, independent of the tillage
137 scenario. This assumption does not affect the results of future projections as we constrain our analysis to
138 cropland that is already cultivated in 2005.

139 Historical simulations were driven using the CRU TS Version 4.03 climate input (Harris et al., 2020) from
140 1901 to 2018. Since this data set does not provide data before 1901, the 30-year climate from 1901 to 1930 was
141 used repeatedly for spin-up simulations covering the period before 1901. Data on $[\text{CO}_2]$ were taken from ice-
142 core measurements (Le Quéré et al., 2015) and the Mauna Loa station (ESRL Global Monitoring Division -
143 Global Greenhouse Gas Reference Network, 2018). Future simulations from 2006-2099 used climate scenarios
144 from four GCMs taken from Coupled Model Intercomparison Project Phase 5 (CMIP5) in bias-adjusted as
145 provided by the ISIMIP2b project (Frieler et al., 2017; Hempel et al., 2013): HadGEM2-ES, GFDL-ESM2M,
146 IPSL-CM5A-LR and MIROC5 for both a weak climate forcing (Representative Concentration Pathway (RCP)
147 2.6) and a strong climate forcing (RCP8.5) with corresponding $[\text{CO}_2]$ levels. The GCM data sets provide inputs
148 for air temperature, precipitation, radiation, and $[\text{CO}_2]$. The historic period for these GCM-specific simulations
149 was based on bias-adjusted data from the GCMs rather than on CRU data, to avoid inconsistencies at the
150 transition between historic and future periods. Land-use change in the future was not analyzed in this context, as
151 the SOC potential of the current agricultural area was the focus of this investigation so that land-use patterns
152 after 2005 were held constant after 2005. All results are presented as averages across the ensemble of climate
153 models per RCP, unless stated otherwise. Additional simulations with constant $[\text{CO}_2]$ for both RCP2.6 and
154 RCP8.5 allow for the isolation of CO_2 fertilization effects. Conventional tillage starts in 1700. For the period



155 1700-1850, the residue extraction rate of the year 1850 is assumed. For conventional tillage, the default value of
156 tillage intensity is set to 0.9 and the fraction of residues submerged by tillage to 0.95. The fraction of residues
157 that are harvested in case of residue extraction is 70% of all above-ground residues (with the remaining 30% of
158 above-ground residues and all roots left on the field). In the case without residue harvest, 100% are left on the
159 field and only the harvested organs (e.g. grains) are removed.

160 2.4 Data analysis and metrics

161 Our analysis is based on simulated changes in cropland SOC stocks as well as the contributing processes,
162 including the turnover rate, heterotrophic respiration, litterfall, and the net primary production (NPP) of cropland
163 areas. NPP is calculated following Schaphoff et al. (2018).

164 The turnover rate for cropland is calculated as:

$$165 \quad mtr_{SOC,agr} = \frac{rh_{agr}}{SOC_{agr}} * 100, \quad (1)$$

166 with $mtr_{SOC,agr}$ as the mean turnover rate for cropland SOC ($\% a^{-1}$), SOC_{agr} is the SOC content for cropland (g)
167 and rh_{agr} is the heterotrophic respiration for cropland ($g a^{-1}$).

168 Decomposition of organic matter pools is following the first-order kinetics described in Sitch et al., (2003). Total
169 heterotrophic respiration (R_h) accounts for 60% of directly decomposed litter ($R_{h,litter}$) and respiration of the fast
170 and slow soil pools (decomposition rate of $0.03 a^{-1}$ and $0.001 a^{-1}$, respectively). From the 40% remaining litter
171 pool, 98.5% are transferred to the fast soil C pool and 1.5% to the slow soil C pool:

$$172 \quad R_{h,agr} = R_{h,litter,agr} + R_{h,fastSoil,agr} + R_{h,slowSoil,agr}, \quad (2)$$

173 Cropland litterfall ($C_{litterfall,agr}$) in $g C a^{-1}$ is calculated by considering root, stem, and leaf carbon in dependency of
174 residue recycling shares:

$$175 \quad C_{litterfall,agr} = (C_{root,CFT} + ((C_{leaf,CFT} + C_{stem,CFT}) \cdot f_{res,CFT})) \cdot f_{cell,agr}, \quad (3)$$

176 with $C_{root,CFT}$ being the C pools of crop roots per CFT, $C_{leaf,PFT}$ the C pool of crop leaves per CFT, $C_{stem,PFT}$ the
177 stems and mobile reserves per CFT, $f_{res,CFT}$ the residue fraction which is returned to the soil per CFT and $f_{cell,agr}$
178 the fraction of agricultural area of the cell. To calculate the historical losses of SOC from land-use change, the
179 fraction of SOC under PNV, which will become cropland in the future combined with the historical cropland
180 SOC parts are calculated as:

$$181 \quad SOC_{LUC,t} = d_{SOC,pnv,t} \cdot (area_{agr,2005} - area_{agr,t}) + d_{SOC,agr,t} \cdot area_{agr,t}, \quad (4)$$



182 where $d_{SOC,pnv,t}$ is the SOC density (g m^{-2}) for PNV area at time step t , which will become cropland in the
183 future, calculated as:

$$184 \quad d_{SOC,pnv,t} = \frac{d_{SOC,cell,t} \cdot area_{cell} - d_{SOC,agr,t} \cdot area_{agr,t}}{area_{pnv,t}} \quad (5)$$

185 where $d_{SOC,pnv,t}$, $d_{SOC,cell,t}$, $d_{SOC,agr,t}$ are the SOC densities (g m^{-2}) for the PNV part within the cell, the density
186 for the entire cell, and the agricultural part within the cell, respectively, at time step t (year), $area_{pnv,t}$ and
187 $area_{agr,t}$ are the corresponding areas of PNV and agriculture (m^2) at time step t and $area_{cell}$ is the area of the
188 entire cell, which does not change over time. We considered different climatic regions such as tropical wet,
189 tropical moist, tropical dry, warm temperate moist, warm temperate dry, cold temperate moist, cold temperate
190 dry, boreal moist, and boreal dry regions, following the IPCC climate zone classification (IPCC, 2006a, Fig. S1
191 in the appendix), using averaged climate inputs for the period between the year 2000 and 2009. Polar dry, polar
192 moist, and tropical montane regions were excluded from this analysis, as these regions do not include any
193 cropland.

194 3 Model performance

195 Modeled global average SOC stocks (period 2000-2009 and year 2018) are compared with previous model
196 versions and literature estimates (Table 2). Simulated SOC stocks in LPJmL5.0-tillage2 exhibit higher SOC
197 content compared to the LPJmL5.0 (von Bloh et al., 2018) model version and LPJ-GUESS (Olin et al., 2015),
198 with total average global SOC stocks of 2640 Pg C for simulations with land use (h_dLU) and 2940 Pg C for
199 simulation with PNV only and no land use (h_PNV). The simulated stocks correspond well to estimates by
200 Carvalhais et al. (2014) for global averages but are lower for cropland SOC stocks. Total SOC stocks simulated
201 by LPJmL5.0-tillage2 are 2640 Pg for the entire soil column of 3 m, which are 300 Pg higher than estimates
202 provided by Jobbágy and Jackson (2000). Global SOC for PNV is 2580 Pg for the upper 2 m, which compares
203 well with estimates between 2376 Pg to 2476 Pg provided by Batjes (1996), who reported SOC stocks for the
204 upper 2 m of soil. Global average cropland SOC stocks between the year 2000 and 2009 as well as for the year
205 2018 for the entire soil column are estimated to be 170 Pg C, which is higher than estimates of 148-151 Pg C by
206 Olin et al. (2015). Zomer et al. (2017) reported cropland SOC stocks of 140 Pg C for the upper 0.3 m of soil,
207 which are higher than the cropland SOC stocks of 75 Pg C simulated for the upper 0.3 m in LPJmL. Ren et al.
208 (2020) reported cropland SOC stocks for the first 0.5 m of soil to be 115 Pg C for the period 2000-2010, which is
209 higher than cropland SOC of 95 Pg C for the upper 0.5 m in LPJmL. Scharlemann et al. (2014) conducted a
210 literature review on global SOC stock and found a wide range of estimates (504-3000 Pg C) and variability
211 across time and space and a high dependency on soil depth, with a median global SOC stock of 1460 Pg C.
212 Generally simulated SOC stocks by LPJmL5.0-tillage2 correspond well with literature and other model
213 estimates.



214 **Table 2: Global SOC pools (Pg C) for the LPJmL5.1-tillage2, LPJmL5.0, and LPJ-GUESS model compared to**
 215 **literature estimates. Values are averages for the period 2000-2009, for the year 2018, and the upper 0.3, 1, and 2 m of**
 216 **soil. PNV values are simulations with potential natural vegetation only (no land use), global SOC average includes**
 217 **PNV and land use.**

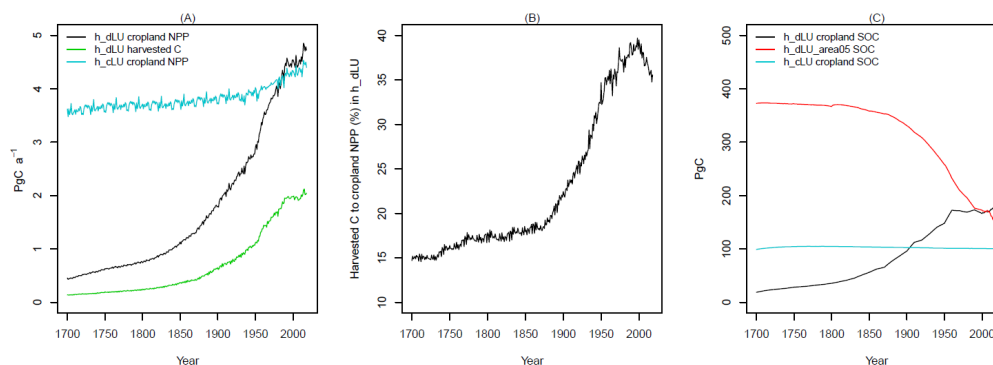
| | Model estimates | | | Literature estimates | | | | |
|---------------------|---|----------------------------------|-------------------------------|--|--|--|--------------------|---|
| | LPJmL5.0-tillage2 (this study) | LPJmL5.0 (von Bloh et al., 2018) | LPJ-GUESS (Olin et al., 2015) | Carvalhais et al., 2014 | Batjes, 1996 | Jobbágy and Jackson, 2000 | Zomer et al., 2017 | Scharlemann et al., 2014 |
| Global SOC PNV only | 2940 ^{1a} 2960 ^{2a} 2580 ^{b1} , 2185 ^{c1} , 1555 ^{d1} | 2344 ^{1a} | 1671 ³ | - | 2376 ^{b4} – 2476 ^{b4} | - | - | - |
| Global SOC average | 2640 ^{1a} 2645 ^{2a} 2295 ^{b1} , 1910 ^{c1} , 1300 ^{d1} | 2049 ^{1a} | 1668 ³ | 2397 ⁴ (1837 ^x - 3257 ^y) | - | 1933 ^b , 2344 ^a | - | 1460 (504 ^d – 3000 ^e) |
| Cropland SOC | 170 ^{1a} 170 ^{2a} 145 ^{b1} , 115 ^{c1} , 75 ^{d1} , | - | 148 ³ | 327 ⁴ (242 ^x - 460 ^y) | - | 210 ^b , 248 ^a | 140 ^d | - |

218 Values are estimates for: ^a entire soil column, ^b upper 2m of soil, ^c upper 1m of soil, ^d upper 0.3m of soil, ^e not indicated.
 219 Year of estimate value: ¹ 2000-2009, ² 2018, ³ 1996-2005, ⁴ not indicated. ^x 2.5th percentile, ^y 97.5th percent

220 4 Results

221 4.1 Historical development of cropland NPP and SOC stocks

222 During the simulation period, cropland NPP increases in the dynamic LU simulation (h_dLU) from 0.7 Pg C a⁻¹
 223 in 1700 to 4.7 Pg C a⁻¹ in 2018, while cropland SOC increases from 18 Pg C to a total of 171 Pg C (Fig. 2A and
 224 2C) in the year 2018. The increase in cropland SOC can be explained by an increase in cropland area (Fig. S2B
 225 in the appendix). During the same time, harvested C increases from 0.1 Pg C a⁻¹ to 2.0 Pg C a⁻¹. The ratio of
 226 harvested C to cropland NPP increases with time, especially after the year 1900 (Fig. 2B), as more material is
 227 harvested compared to cropland NPP. The aggregated SOC stock on all land that is cropland in the year 2005
 228 declines substantially, especially after the year 1900 (red line in Fig. 2C), which reflects the decline in cropland
 229 SOC density (Fig. S2A in the appendix). We also find that cropland SOC density steadily increases between
 230 1700 and 1950, and decreases since 1950 (Fig. S2A in the appendix). Simulations with a constant land use
 231 pattern of 2005 (h_cLU) for cropland NPP and cropland SOC show no substantial dynamics (Fig. 2A and C).
 232 These simulations are not entirely insightful, because they do not account for the historical increase in inputs,
 233 e.g. fertilizer.



234

235 **Figure 2: Plots for cropland NPP and harvested C (A), percentage of harvested C to cropland NPP in h_dLU (B) and**
236 **SOC for cropland stocks, and historical SOC losses from LUC (C) for the years 1700-2018 for simulations with**
237 **transient land use (h_dLU), constant land use of 2005 (h_cLU), transient land use and SOC development from land-**
238 **use change including cropland area and historical PNV area which will be converted until the year 2005**
239 **(h_dLU_area05).**

240 In contrast to the scenario with dynamic land use and the ones with constant land use, the h_dLU_area05
241 scenario describes a combination of historical cropland SOC and historical SOC of natural vegetation, which is
242 or has been cropland until the year 2005. This describes the SOC dynamics of all land that is subject to the
243 historical land-use change (LUC) (Fig. 2C). Loss of historical SOC is calculated as the difference between the
244 years 1700 and 2018 on the land area that was cropland at any point in time (Fig. 2C, red line). Through this
245 approach, we calculate a total historical SOC loss of 215 Pg C. Cropland SOC stocks are increasing over time
246 (Fig. 2C, black line), reflecting the increase of cropland area. PNV has a higher SOC density, and therefore SOC
247 stock, before the conversion to cropland (Fig. S2A in the appendix). Only when the area which is converted at
248 any time to cropland is considered over the entire period, the calculation of the actual decrease in SOC stocks
249 from LUC is possible (Fig. 2C, red line).

250 4.2 Future soil carbon development with idealized management under climate change

251 Future cropland SOC stock development was analyzed considering two different radiative forcing pathways
252 (RCPs) with four different climate scenarios (GCMs) per RCP and four idealized management assumptions
253 (Table 2). To estimate the SOC sequestration potential on current cropland and to exclude the influence from
254 LUC, the cropland area was kept constant at the year 2005 pattern. Results for future SOC development show
255 that the maximum decrease in SOC stocks on current global cropland area between the year 2005 until the end of
256 the century occurs in the scenario with no-till applied on global cropland, no residues retained and RCP8.5
257 climate (NT_NR_85). Total cropland SOC loss for this scenario is evaluated as 38.4 Pg C, or 28.1% in relative
258 terms compared to the SOC stocks in the year 2005. All management systems, which extract residue from the
259 field, show a strong decrease in cropland SOC stocks, independent of the climate scenario (Fig. 3B). Differences
260 for cropland SOC development between different tillage systems as well as between the two radiative forcing



261 pathways RCP2.6 and RCP8.5 are small. Management systems, which retain residue on the field after harvest,
 262 show the smallest reduction in cropland SOC stocks, with a maximum reduction of 5.1 Pg C (equivalent to 3.8%
 263 decline) in the T_R_26 management system. Differences between GCM-specific climate scenarios or radiative
 264 forcing pathways (RCPs) were small in comparison to differences in residue management assumptions for SOC,
 265 turnover rates, and litterfall rates (Fig. 3) but larger than differences in assumptions on tillage systems. Only for
 266 agricultural NPP (Fig. 3A), differences in radiative forcing pathways were the main determinant of NPP
 267 dynamics, followed by GCM-specific climate scenarios.

268 **Table 3: Summary of absolute and relative global cropland SOC stock change between the years 2006 and 2099 for**
 269 **different management systems for RCP2.5 and RCP8.5 as averages across all four GCMs.**

| Management | Absolute cropland SOC change 2006 – 2099 (Pg C) | | Relative cropland SOC change 2006 – 2099 (%) | |
|------------|--|--------|---|--------|
| | RCP2.6 | RCP8.5 | RCP2.6 | RCP8.5 |
| | T_R | -5.1 | -4.4 | -3.8 |
| T_NR | -37.6 | -38.1 | -27.5 | -27.8 |
| NT_R | -3.6 | -3.2 | -2.6 | -2.3 |
| NT_NR | -37.8 | -38.4 | -27.7 | -28.1 |
| TRc05 | -24.1 | -24.0 | -17.6 | -17.6 |

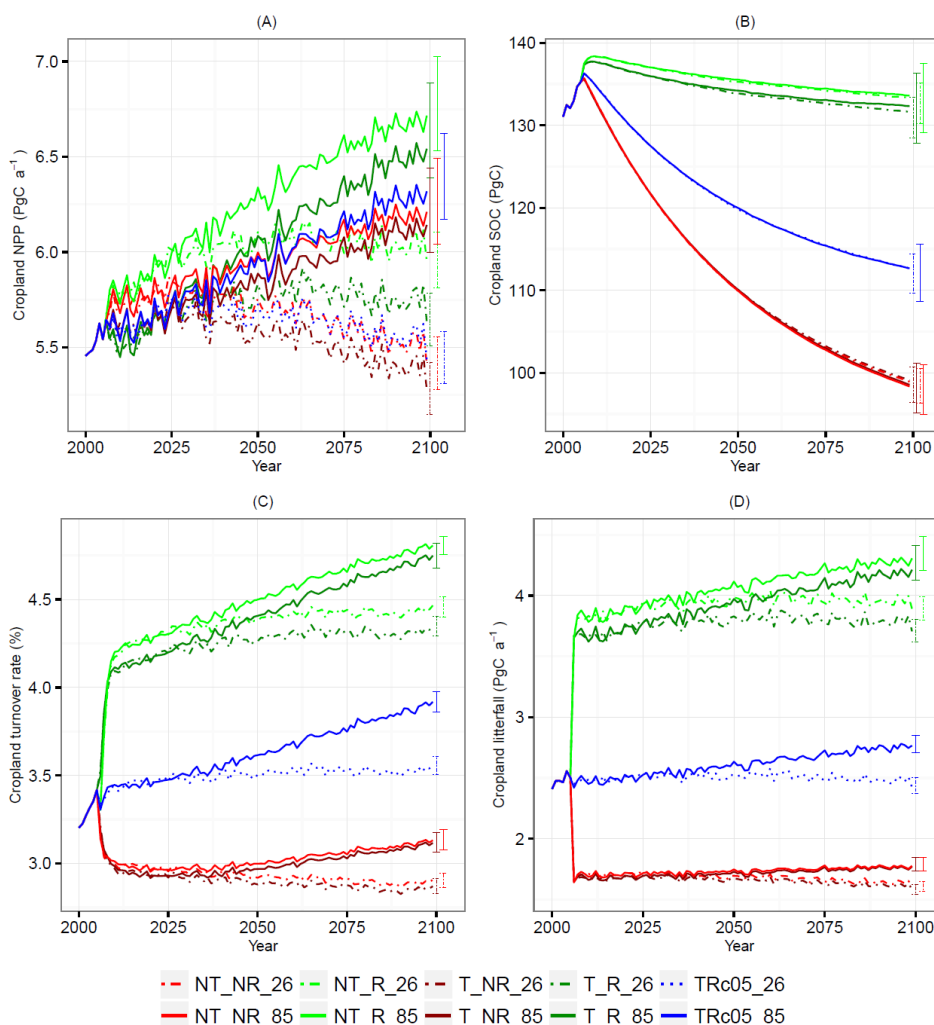


Figure 3: Global sums for cropland for NPP (A), SOC (B), turnover rate (C), and litterfall (D) from 2000-2005 for default management inputs and from 2006-2099 under constant cropland area of 2005 for five different management scenarios and two RCPs. Presented are the mean values across all four GCMs as lines. The spread across all GCMs is depicted as bars in the year 2100. The numbers ₂₆ and ₈₅ describe the climate forcing RCP2.6 (e.g. TRc05₂₆) and RCP8.5 (e.g. TRc05₈₅). Green – residues retained (R), red – residues removed (NR), dashed – RCP2.6, solid – RCP8.5, light color – no-till (NT), dark color – tillage (T). Tillage and residue management held constant at 2005 level in TRc05; tillage and residues left on the field (T_R), tillage and residues removed (T_{NR}), no-till plus residues left on the field (NT_R) and no-till and residues removed (NT_{NR}).

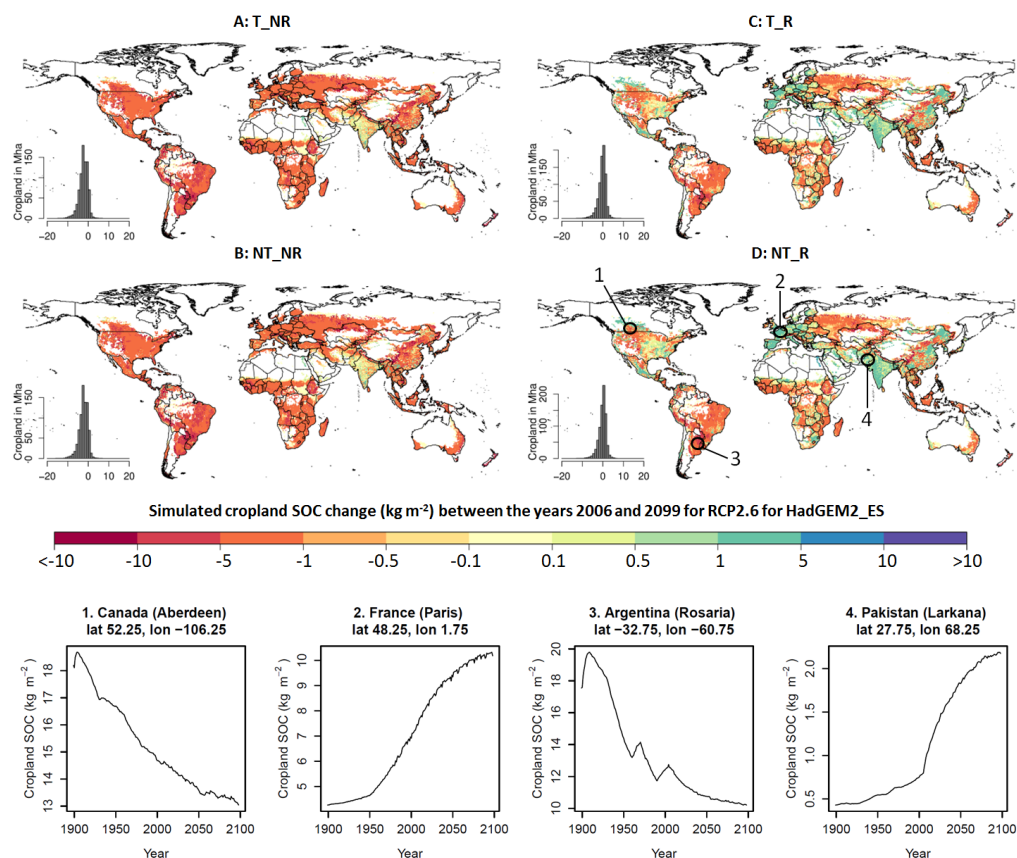
Stocks of cropland SOC and turnover rates (Fig. 3C) initially increase in systems that retain residues, such as T_R and NT_R, after the change in management after the year 2005 (Fig. 3B and C), as more residual C is added to the soil column in comparison to the historic residue removal rates (Fig. 3D).



283 Turnover rates are higher for the high radiative forcing pathway RCP8.5 in comparison to RCP2.6. The
284 simulated cropland NPP (Fig. 3A) is sensitive to the radiative forcing, as the level of NPP is higher in the high-
285 end RCP8.5 scenario, and lower in the lower-end RCP2.6 scenario. This is because of the strong response of
286 NPP to CO₂ fertilization, which overcompensates the climate-driven reduction in NPP (compare Fig. S3 in the
287 appendix). NPP is less sensitive to the assumptions on tillage practices in comparison to the effects of
288 assumptions on residue management. NT_R results in the highest NPP mainly due to water-saving effects, which
289 are caused by the surface litter cover, which reduces evaporation from the soil surface and at the same time
290 increase infiltration of water into the soil. NPP increases steadily until 2099 in RCP8.5 scenarios, because of the
291 CO₂ fertilization effects (compare Fig. S3 in the appendix). In RCP2.6, NPP first slightly increases and then
292 decreases until the end of the century in all tillage and residue scenarios. However the ranking of management
293 effects is insensitive to the radiative forcing pathway: NT_R results in the highest NPP, T_NR in the lowest
294 values.

295 **4.3 Regional cropland SOC analysis**

296 Simulation results show that globally aggregated SOC stocks on current cropland decline until the end of the
297 century for all management systems, but there are regional differences (Fig. 4). We find that in some regions,
298 cropland SOC can increase until the end of the century, even though global sums indicate a total decline. For
299 cropland SOC density, increases between the years 2006 and 2099 can be found for T_R and NT_R management
300 systems for more than 1/3 of the global cropland area, most clearly in regions in Europe, India, Pakistan,
301 Afghanistan, southern Chile, southern Mexico, eastern China and south-eastern USA (Fig. 4C and D).
302 Historically, regions which already showed an increase in cropland SOC density since 1900 until today, such as
303 in France or Pakistan, or a decrease, such as Canada and Argentina, tend to continue this development also in the
304 future (see plots in Fig. 4 for exemplary cells). In systems in which residues are not returned to the soil (T_NR
305 and NT_NR), global cropland SOC density change is dominated by a decline.



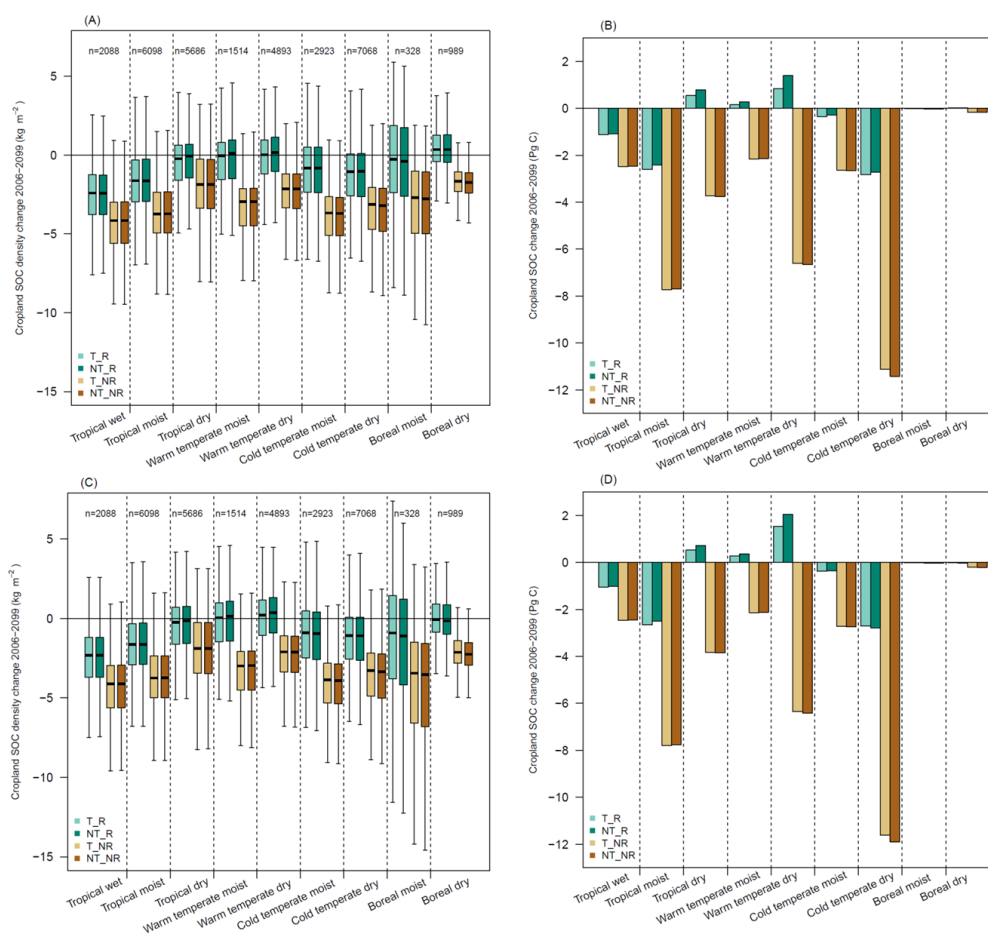
306

307 **Figure 4: Simulated cropland SOC change (kg m^{-2}) between the years 2006 and 2099 (kg m^{-2}) for RCP2.6 for GCM**
 308 **HadGEM2-ES for the four different management options (T_R, NT_R, T_NR, and NT_NR). The plots 1.-4. show**
 309 **examples of SOC development (kg m^{-2}) from the year 1900 to 2099 for different explanatory regions as shown on map**
 310 **D (NT_R). The difference maps of affected change categories between RCP2.6 and RCP8.5 are shown in Fig. 5. Maps**
 311 **for GFDL-ESM2M, IPSL-CM5A-LR and MIROC5, and RCP8.5 are in the appendix (Fig. S7 to S13).**

312 Results for different climatic regions suggest that the difference between RCP2.6 and RCP8.5 radiative
 313 forcing only plays a minor role for cropland SOC stock development (Fig. 5). Findings suggested that a positive
 314 median increase in cropland SOC density between the years 2006 and 2099 can be found in warm temperate
 315 moist, warm temperate dry, and boreal regions for RCP2.6 (GCM average) for T_R and NT_R management
 316 systems (Fig. 5B). The total aggregated cropland SOC change for each climate region depends on the cropland
 317 extent of the region. The smallest amounts of cropland are found in boreal moist and dry regions, which results
 318 in a total cropland SOC stock change of negligible size (Fig. 5B and D). Total increases in cropland SOC stocks
 319 can be found for both RCP2.6 (Fig. 5A and B) and RCP8.5 (GCM average) (Fig. 5C and D) for tropical dry,
 320 warm temperate moist, and warm temperate dry regions in T_R and NT_R management systems. For all regions



321 across all simulations, management systems in which residues are not returned to the soil, cropland SOC stocks
 322 decrease. The highest absolute losses of total cropland SOC stocks for these systems (T_NR and NT_NR) can be
 323 found in cold temperate dry climates, followed by tropical moist and warm temperate dry regions, which are the
 324 regions with major cropland shares.



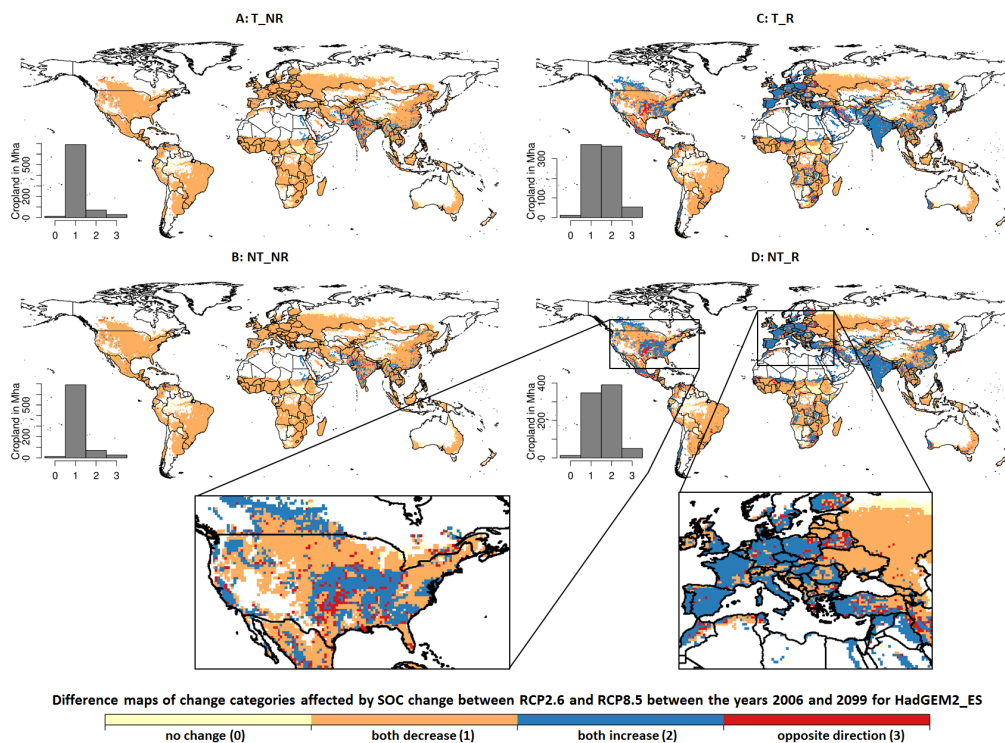
325

326 **Figure 5: Boxplots of cropland SOC density change (kg m⁻²) and bar plots of total cropland SOC change (Pg C)**
 327 **between the years 2006 and 2099, averaged across the four GCMs (HadGEM2_ES, GFDL-ESM2M, IPSL-CM5A-LR,**
 328 **MIROC5) in RCP2.6 (A and B) and RCP8.5 (C and D) for the climatic regions classified by the IPCC (2006) and the**
 329 **four management systems T_R, NT_R, T_NR, and NT_NR. The same plots for each GCM can be found in Fig. S5 and**
 330 **S6 in the appendix, n is the number of cropland cells included in each climate region.**

331 Regional results also indicate stronger differences between GCM-specific climate scenarios within the same
 332 radiative forcing pathway (RCP). The highest positive cropland SOC stock response can be found for GCM



333 GFDL-ESM2M in both RCP2.6 and RCP8.5 for T_R and NT_R for warm temperate dry climates, while the
 334 positive response for tropical dry and warm temperate moist climates is lower compared to the other three GCMs
 335 (compare Fig. S5D and S6D in the appendix). Results for the IPSL-CM5A-LR climate scenarios for both
 336 RCP2.6 and RCP8.5 generally show the most negative response for cropland SOC density change and cropland
 337 SOC stock change, followed by HadGEM2_ES.



338

339 **Figure 6: Difference maps of change categories for cropland SOC density change between both RCP2.6 and RCP8.5**
 340 **from the year 2006 until 2009 for GCM HadGEM_ES in each management system. Orange areas indicate a reduction**
 341 **in cropland SOC density between the years 2006 and 2009 in both RCPs, blue areas show an increase in SOC density,**
 342 **in light yellow areas no change occurs, and for red, SOC density change occurs in opposite directions in RCP2.6 and**
 343 **RCP8.5. The numbers in brackets (0) to (3) correspond to the categories in the histogram.**

344 The comparison of cropland affected in RCP2.6 and RCP8.5 indicates that most regions show effects with
 345 the same direction of response in SOC density, so either it decreases or increases in both RCP2.6 and RCP8.5,
 346 which is highlighted by the blue and orange regions in Fig. 6. Red cells, which indicate that the effects in both
 347 RCPs go in the opposite direction can only be found in a few regions, e.g. the United States and Turkey. In total,
 348 between 50 and 53 million hectares (Mha) of cropland shows the opposite directions globally for the NT_R and
 349 T_R, while this is halved (between 27 and 29 Mha) for T_NR and the NT_NR management system.



350 **5 Discussion**

351 **5.1 SOC development in the past and losses due to land-use change**

352 Historical simulations show that the conversion of natural land to cropland has caused SOC losses of 215 Pg C
353 between the year 1700 and 2018 (Fig. 2C). Soil C density and NPP in natural vegetation are higher compared to
354 those found in croplands, which results in C losses after conversion of natural land to cropland. NPP in croplands
355 is often lower compared to NPP in natural vegetation, as the cultivated period is typically shorter than the
356 vegetative period in which natural vegetation is productive so that cultivated plants have less time to accumulate
357 C. Further, cropland is cultivated and crops are harvested, which results in the extraction of NPP in form of
358 harvested material, which leads to a further decline of SOC stocks. Cropland expansion is the main driver for
359 increases in total cropland SOC stocks, as cropland SOC density steadily increased since the year 1700 starting
360 at 7 kg m⁻² and reaching its maximum in the year 1960 at 13 kg m⁻², but since then cropland SOC density
361 decreased, down to 11 kg m⁻² today (Fig. S2A in the appendix). SOC density on cropland showed this trend,
362 even though fertilizer use increased since the 1960s, which was found to be able to promote SOC sequestration,
363 especially in temperate regions (Alvarez, 2005). Since the 1960s, cropland expansion has slowed down, but
364 global yields have, on average, more than doubled (Pingali, 2012; Ray et al., 2012; Wik et al., 2008). Ren et al.
365 (2020) show that historical cropland SOC increase was mainly attributed to cropland expansion, which is in
366 agreement with the findings here. The ratio of harvested C to cropland NPP increases with time (Fig. 2B) so that
367 the increase in yields does not have a positive effect on cropland SOC, as more and more C is extracted from the
368 soil in the form of harvested material.

369 It was estimated that conversion of natural land to cultivated land can result in SOC loss of up to 30 to 50%
370 (Lal, 2001). Sanderman et al. (2017) estimated historical global SOC losses of natural land to cropland
371 conversion by 133 Pg C, of which most of the losses occurred in the last 200 years. Pugh et al. (2015) modeled
372 C emissions from LUC accounting for agricultural management, such as harvesting and tillage, and found
373 maximum C losses in vegetation and SOC by 225 Pg C since the year 1850. Le Quéré et al. (2018) also
374 estimated the C flux to the atmosphere due to LUC, including deforestation, to be 235 Pg C (\pm 95) since the year
375 1750.

376 **5.2 Future cropland SOC development on current global cropland**

377 Future SOC stocks on current cropland depend on climate and management. We find that current cropland
378 remains to be a source of C, even though the decline of SOC on current cropland can be reduced through
379 management. The most efficient measure to reduce SOC losses on cropland is residue management. The amount
380 of residues that can be retained on cropland depends on productivity. At the same time, the addition of fresh
381 material increases the turnover rate in the soil, as this material is more easily decomposed than the remaining
382 SOC stocks from the historical natural ecosystems.

383 The different management aspects show the same ranking in importance under both radiative forcing
384 pathways and the changes on cropland SOC only differ slightly. Cropland SOC stocks at the end of the century



385 vary only between those two RCPs between -0.6% and +0.6% for all four management systems. This is caused
386 by a compensating effect of higher productivity by elevated CO₂ under RCP8.5, which counteracts the increase
387 in turnover rates at higher temperatures (see Fig. S3 in the appendix for comparison with constant [CO₂]
388 simulations).

389 Even though experiments have shown that tillage can reduce SOC stocks significantly compared to no-till
390 (Abdalla et al., 2016; Kurothe et al., 2014), tillage management only has small effects on aggregated global
391 cropland SOC in our simulations. Tillage practices account for differences in cropland SOC stocks of 0.9% and
392 1.3% between T_R vs. NT_R in 2099 for RCP8.5 and RCP2.6, respectively, and less than 0.2% between T_NR
393 vs. NT_NR for both RCPs. Differences in SOC stocks on cropland between the tillage systems decrease if
394 residues are not retained on the field. NPP responds more strongly to the tillage system, which is likely to be
395 driven by secondary effects (e.g. no-till increases soil moisture and nutrient availability from mineralization), but
396 shows no long-term effect on SOC stock development.

397 With the given complexity in responses to tillage, the application of no-tillage has been discussed
398 ambiguously in the literature (Chi et al., 2016; Derpsch et al., 2014, 2010; Dignac et al., 2017; Powlson et al.,
399 2014). The LPJmL5.0-tillage model is well capable of reproducing these process interactions and diversity in
400 results (Lutz et al. 2019). Tillage systems thus need to be selected based on local conditions, but we find these to
401 be less important than residue management. Given this dependency of the SOC accumulation potential on
402 climatic and management conditions, there are strong regional differences in the response of SOC to changes in
403 management. In line with Stella et al. (2019), who investigated the contribution of crop residues to cropland
404 SOC conservation in Germany and found a decrease in SOC stocks until 2050, if residues are not returned to the
405 soil, we find that large parts of western Europe can indeed increase the SOC stocks under management systems
406 in which residues are retained on the field. Zomer et al. (2017) analyzed the global sequestration potential for
407 SOC increase in cropland soils and found the highest potentials in India, Europe, and mid-west USA, results
408 which correspond well with our findings. Also, the duration of the historical cultivation of the cropland is an
409 important aspect in the ability to sequester C in current cropland soils. Stella et al. (2019) find the highest SOC
410 sequestration potentials in soils with low SOC stocks (i.e. in highly degraded soils).

411 **5.3 Potential for SOC sequestration on cropland and recommendations for future analysis**

412 For the past years, there has been an ongoing debate on how much SOC can be stored in agricultural soils
413 through adequate management as a climate change mitigation strategy (Baker et al., 2007; Batjes, 1998; Lal,
414 2004; Luo et al., 2010; Stockmann et al., 2013). For example, globally applied no-till management on cropland
415 was estimated to have a SOC sequestration potential of 0.4-0.6 Gt CO₂ a⁻¹ (Powlson et al., 2014). Additionally,
416 the sequestration of SOC can be beneficial to soil quality and productivity and minimize soil degradation (Lal,
417 2009, 2004). In our simulations with LPJmL5.0-tillage2, we find that on current cropland, these sequestration
418 potentials cannot be achieved by varying tillage practices and residue removal rates, even though the residue
419 management system is important for cropland SOC dynamics.



420 There is a general uncertainty in how experimental findings can be scaled up, as e.g. demonstrated by a
421 review conducted by Fuss et al. (2018). While process-based modeling as applied here can take environmental
422 conditions into account and can compare different management aspects, it is still subject to various uncertainties.
423 One crucial aspect is the history of land-use systems, including the trend in land productivity. Karstens et al.
424 (2020, under review) show that the historical intensification of cropland could already have converted the
425 cropland to a net carbon sink, but rely on an assumption that residue amounts scale linearly with productivity,
426 which is not always true, e.g. when breeding of dwarf varieties that lead to changing allometries and yield
427 formation (Subira et al., 2016). Depending on the agricultural management option, it is argued that the maximum
428 sequestration potential is reached after the soil has a new higher equilibrium state, which can be reached after 10-
429 100 years, depending on climate, soil type, and SOC sequestration option (Smith, 2016). The IPCC suggests a
430 default saturation time of the soil sink of 20 years, after which the equilibrium is reached, which then has to be
431 maintained to avoid additional release of CO₂ (IPCC, 2006). Increasing cropland SOC in a first step can be
432 achieved by adding more C to the soil than is lost by respiration, decomposition and harvest, and soil
433 disturbance. Maintaining SOC levels on cropland after the soil has reached a new equilibrium will require the
434 application of management strategies that do not deplete SOC. The ‘4 per 1000’ initiative requires annual SOC
435 sequestration on croplands of approximately 2 to 3 Pg C a⁻¹ in the top 1m of cropland soils, which was criticized
436 to be unrealistic (de Vries, 2018; White et al., 2018). In this analysis, only two management options affecting
437 SOC, tillage treatment and residues management, are considered. High SOC sequestration potentials on cropland
438 are argued to be only achieved by applying a variety of management options, e.g. additional restoration of
439 degraded land (Griscom et al., 2017; Lal, 2003), agroforestry (Lorenz and Lal, 2014; Torres et al., 2010), biochar
440 (Smith, 2016), bio-waste compost (Mekki et al., 2019), which add forms of organic material which increase
441 turnover times of SOC. A combination of these different practices is more likely to achieve higher SOC
442 sequestration rates on cropland (Fuss et al., 2018). Management options that aim at increasing SOC may also
443 affect yields, as they can maintain productivity and ensure yield stability (Pan et al., 2009), but reductions in
444 SOC can also reduce yields substantially (Basso et al., 2018). Similarly, the intensification of cropland
445 productivity can have substantial effects on cropland SOC if the additional productivity also increases litterfall
446 rates (Karstens et al., 2020 - under review). Yet, the productivity increase can come with an even stronger
447 increase in harvested material, as here demonstrated, which can lead to a reduction in total cropland SOC. The
448 conversion from natural land to cropland typically causes substantial SOC losses, which stresses the need to
449 further limit land-use expansion and thus requires an intensification of land productivity on current cropland. In
450 our analysis, we did not account for the effects of future LUC, but projections show an increase in total cropland
451 area in the future (Stehfest et al., 2019), so that global SOC is expected to further decline.

452 Further research of agricultural management practices that influence SOC development at the global scale
453 should investigate the impact of cover crops, rotations, and optimal cultivar choice per region and location (e.g.
454 Minoli et al., 2019) and different options for cropland intensification (e.g. Gerten et al., 2020) in a more explicit
455 manner. SOC stabilization mechanisms, such as clay mineral protection and forming of macroaggregates in no-
456 till managed soils (Luo et al., 2016), effects of microorganisms, such as N-fixation and phosphorous acquisition



457 from fungi and bacteria, which also regulate plant productivity and community dynamics (Heijden et al., 2008),
458 as well as effects of soil structure (Bronick and Lal, 2005) on SOC dynamics have not been considered here or in
459 other global process-based assessments and should be taken into account. Plants and associated root systems can
460 reduce surface erosion and water runoff (Gyssels et al., 2005), but losses of SOC from runoff and increased
461 erosion (Kurothe et al., 2014; Naipal et al., 2018) are not considered here either. Residues from plants can
462 influence labile, intermediate, and stable SOC pools through the C:N ratio. Residues with high C:N ratios (e.g.
463 straw) decomposed relatively slow and can increase SOC, but reduce N availability to the plants, while residues
464 with low C:N decompose relatively fast and can release N to the soil through mineralization (Macdonald et al.,
465 2018). The speed of residue decomposition can also influence the effectiveness of residues as a soil cover, with
466 effects on soil moisture through infiltration. Impacts of biodiversity and living fauna such as microorganisms on
467 SOC sequestration is not modeled in this analysis, even though they are recognized to have a substantial
468 influence on the dynamics of SOC (Chevallier et al., 2001).

469 The implementation of such effects is desirable but needs to be assessed with respect to the process
470 understanding, the availability of input data at the global scale, and the availability of modeling approaches (Lutz
471 et al., 2019a). Global-scale modeling approaches, in comparison to local or regional studies, allow for the
472 possibility to identify regional patterns related to SOC sequestration responses with the potential to foster
473 experimental studies in areas so far not investigated, but relevant for global assessments (Luo et al., 2016;
474 Nishina et al., 2014). They are needed to upscale findings from experimental sites so that the potential of such
475 measures for climate change mitigation can be better understood and climate protection plans are made with
476 better estimates.

477 **6 Conclusion**

478 In conclusion, the here analyzed agricultural management systems are not sufficient to increase global SOC
479 stocks on current cropland until the end of the 21st century. The interaction of SOC sequestration and cropland
480 productivity needs to be better disentangled. Additional C inputs from e.g. manure, cover crops, and rotations are
481 needed and could offset further SOC losses, but additional research on the potentials of these cropland
482 management options and available amounts that could be applied is needed. We find that the potential for SOC
483 sequestration on current global cropland is too small to fulfill expectations as a negative emission technology,
484 which stresses the importance to reduce GHG emissions more strictly by other means, to reach climate
485 protection targets as outlined in the 2015 Paris Agreement.

486 **Code and data availability**

487 The source code is available under GNU APGL version 3 license. The exact version of the code described here
488 and the R script used for postprocessing the data from the simulations conducted are archived under
489 <https://doi.org/10.5281/zenodo.4625868> (Herzfeld et al., 2021).

490



491 **Author contributions**

492 TH and CM designed the study in discussion with JH and SR. TH conducted all the model simulations and wrote
493 the paper with support from CM. TH conducted the analysis and prepared all the figures with input from CM and
494 JH. All authors edited the paper.

495 **Competing interests**

496 The authors declare that they have no conflict of interest.

497 **Acknowledgements**

498 TH and SR gratefully thank the German Ministry for Education and Research (BMBF) for funding this work,
499 which is part of the MACMIT project (01LN1317A). JH thanks the BMBF for funding through the SUSTAg
500 project (031b0170A). TH thanks Vera Porwollik for the support in preparing input data sets and code
501 development.

502 **References**

- 503 Abdalla, K., Chivenge, P., Ciais, P., and Chaplot, V.: No-tillage lessens soil CO₂ emissions the most under arid
504 and sandy soil conditions: results from a meta-analysis, 13, 3619–3633, [https://doi.org/10.5194/bg-13-3619-](https://doi.org/10.5194/bg-13-3619-2016)
505 2016, 2016.
- 506 Alvarez, R.: A review of nitrogen fertilizer and conservation tillage effects on soil organic carbon storage, 21,
507 38–52, <https://doi.org/10.1079/SUM2005291>, 2005.
- 508 Baker, J. M., Ochsner, T. E., Venterea, R. T., and Griffis, T. J.: Tillage and soil carbon sequestration—What do
509 we really know?, 118, 1–5, <https://doi.org/10.1016/j.agee.2006.05.014>, 2007.
- 510 Basso, B., Dumont, B., Maestrini, B., Shcherbak, I., Robertson, G. P., Porter, J. R., Smith, P., Paustian, K.,
511 Grace, P. R., Asseng, S., Bassu, S., Biernath, C., Boote, K. J., Cammarano, D., De Sanctis, G., Durand, J.-L.,
512 Ewert, F., Gayler, S., Hyndman, D. W., Kent, J., Martre, P., Nendel, C., Priesack, E., Ripoche, D., Ruane, A. C.,
513 Sharp, J., Thorburn, P. J., Hatfield, J. L., Jones, J. W., and Rosenzweig, C.: Soil Organic Carbon and Nitrogen
514 Feedbacks on Crop Yields under Climate Change, 3, 0, <https://doi.org/10.2134/ael2018.05.0026>, 2018.
- 515 Batjes, N. h.: Total carbon and nitrogen in the soils of the world, 47, 151–163, [https://doi.org/10.1111/j.1365-](https://doi.org/10.1111/j.1365-2389.1996.tb01386.x)
516 2389.1996.tb01386.x, 1996.
- 517 Batjes, N. H.: Mitigation of atmospheric CO₂ concentrations by increased carbon sequestration in the soil, *Biol*
518 *Fertil Soils*, 27, 230–235, <https://doi.org/10.1007/s003740050425>, 1998.
- 519 Batjes, N. H.: Total carbon and nitrogen in the soils of the world, 65, 10–21,
520 https://doi.org/10.1111/ejss.12114_2, 2014.
- 521 von Bloh, W., Schaphoff, S., Müller, C., Rolinski, S., Waha, K., and Zaehle, S.: Implementing the nitrogen cycle
522 into the dynamic global vegetation, hydrology, and crop growth model LPJmL (version 5.0), 11, 2789–2812,
523 <https://doi.org/10.5194/gmd-11-2789-2018>, 2018.
- 524 Bodirsky, B. L., Rolinski, S., Biewald, A., Weindl, I., Popp, A., and Lotze-Campen, H.: Global Food Demand
525 Scenarios for the 21st Century, 10, e0139201, <https://doi.org/10.1371/journal.pone.0139201>, 2015.



- 526 Bronick, C. J. and Lal, R.: Soil structure and management: a review, *Geoderma*, 124, 3–22,
527 <https://doi.org/10.1016/j.geoderma.2004.03.005>, 2005.
- 528 Carvalhais, N., Forkel, M., Khomik, M., Bellarby, J., Jung, M., Migliavacca, M., Mu, M., Saatchi, S., Santoro,
529 M., Thurner, M., Weber, U., Ahrens, B., Beer, C., Cescatti, A., Randerson, J. T., and Reichstein, M.: Global
530 covariation of carbon turnover times with climate in terrestrial ecosystems, 514, 213–217,
531 <https://doi.org/10.1038/nature13731>, 2014.
- 532 Chevallier, T., Blanchart, E., Girardin, C., Mariotti, A., Albrecht, A., and Feller, C.: The role of biological
533 activity (roots, earthworms) in medium-term C dynamics in vertisol under a *Digitaria decumbens* (Gramineae)
534 pasture, 16, 11–21, [https://doi.org/10.1016/S0929-1393\(00\)00102-5](https://doi.org/10.1016/S0929-1393(00)00102-5), 2001.
- 535 Chi, J., Waldo, S., Pressley, S., O’Keeffe, P., Huggins, D., Stöckle, C., Pan, W. L., Brooks, E., and Lamb, B.:
536 Assessing carbon and water dynamics of no-till and conventional tillage cropping systems in the inland Pacific
537 Northwest US using the eddy covariance method, *Agricultural and Forest Meteorology*, 218–219, 37–49,
538 <https://doi.org/10.1016/j.agrformet.2015.11.019>, 2016.
- 539 Derpsch, R., Friedrich, T., Kassam, A., and Hongwen, L.: Current status of adoption of no-till farming in the
540 world and some of its main benefits, 3, 26, 2010.
- 541 Derpsch, R., Franzluebbers, A. J., Duiker, S. W., Reicosky, D. C., Koeller, K., Friedrich, T., Sturny, W. G., Sá,
542 J. C. M., and Weiss, K.: Why do we need to standardize no-tillage research?, 137, 16–22,
543 <https://doi.org/10.1016/j.still.2013.10.002>, 2014.
- 544 Dietrich, J. P., Mishra, A., Weindl, I., Bodirsky, B. L., Wang, X., Baumstark, L., Kreidenweis, U., Klein, D.,
545 Steinmetz, N., Chen, D., Humpenoeder, F., and Wirth, S.: mrland: MadRaT land data package, 2020.
- 546 Dignac, M.-F., Derrien, D., Barré, P., Barot, S., Cécillon, L., Chenu, C., Chevallier, T., Freschet, G. T., Garnier,
547 P., Guenet, B., Hedde, M., Klumpp, K., Lashermes, G., Maron, P.-A., Nunan, N., Roumet, C., and Basile-
548 Doelsch, I.: Increasing soil carbon storage: mechanisms, effects of agricultural practices and proxies. A review,
549 37, <https://doi.org/10.1007/s13593-017-0421-2>, 2017.
- 550 Eyring, V., Bony, S., Meehl, G. A., Senior, C. A., Stevens, B., Stouffer, R. J., and Taylor, K. E.: Overview of the
551 Coupled Model Intercomparison Project Phase 6 (CMIP6) experimental design and organization, *Geosci. Model*
552 *Dev.*, 9, 1937–1958, <https://doi.org/10.5194/gmd-9-1937-2016>, 2016.
- 553 FAO: The State of Food and Agriculture 2019 (SOFA). Moving forward on food loss and waste reduction.,
554 FAO, Rome, Licence: CC BY-NC-SA 3.0 IGO, 2019.
- 555 Forkel, M., Carvalhais, N., Schaphoff, S., v. Bloh, W., Migliavacca, M., Thurner, M., and Thonicke, K.:
556 Identifying environmental controls on vegetation greenness phenology through model–data integration, 11,
557 7025–7050, <https://doi.org/10.5194/bg-11-7025-2014>, 2014.
- 558 Frieler, K., Lange, S., Piontek, F., Reyer, C. P. O., Schewe, J., Warszawski, L., Zhao, F., Chini, L., Denvil, S.,
559 Emanuel, K., Geiger, T., Halladay, K., Hurtt, G., Mengel, M., Murakami, D., Ostberg, S., Popp, A., Riva, R.,
560 Stevanovic, M., Suzuki, T., Volkholz, J., Burke, E., Ciais, P., Ebi, K., Eddy, T. D., Elliott, J., Galbraith, E.,
561 Gosling, S. N., Hattermann, F., Hickler, T., Hinkel, J., Hof, C., Huber, V., Jägermeyr, J., Krysanova, V., Marcé,
562 R., Müller Schmied, H., Mouratiadou, I., Pierson, D., Tittensor, D. P., Vautard, R., van Vliet, M., Biber, M. F.,
563 Betts, R. A., Bodirsky, B. L., Deryng, D., Froking, S., Jones, C. D., Lotze, H. K., Lotze-Campen, H., Sahajpal,
564 R., Thonicke, K., Tian, H., and Yamagata, Y.: Assessing the impacts of 1.5 °C global warming – simulation
565 protocol of the Inter-Sectoral Impact Model Intercomparison Project (ISIMIP2b), 10, 4321–4345,
566 <https://doi.org/10.5194/gmd-10-4321-2017>, 2017.
- 567 Fuss, S., Lamb, W. F., Callaghan, M. W., Hilaire, J., Creutzig, F., Amann, T., Beringer, T., Garcia, W. de O.,
568 Hartmann, J., Khanna, T., Luderer, G., Nemet, G. F., Rogelj, J., Smith, P., Vicente, J. L. V., Wilcox, J.,



- 569 Dominguez, M. del M. Z., and Minx, J. C.: Negative emissions—Part 2: Costs, potentials and side effects,
570 *Environ. Res. Lett.*, 13, 063002, <https://doi.org/10.1088/1748-9326/aabf9f>, 2018.
- 571 Gerten, D., Heck, V., Jägermeyr, J., Bodirsky, B. L., Fetzer, I., Jalava, M., Kumm, M., Lucht, W., Rockström,
572 J., Schaphoff, S., and Schellnhuber, H. J.: Feeding ten billion people is possible within four terrestrial planetary
573 boundaries, 3, 200–208, <https://doi.org/10.1038/s41893-019-0465-1>, 2020.
- 574 Griscom, B. W., Adams, J., Ellis, P. W., Houghton, R. A., Lomax, G., Miteva, D. A., Schlesinger, W. H., Shoch,
575 D., Siikamäki, J. V., Smith, P., Woodbury, P., Zganjar, C., Blackman, A., Campari, J., Conant, R. T., Delgado,
576 C., Elias, P., Gopalakrishna, T., Hamsik, M. R., Herrero, M., Kiesecker, J., Landis, E., Laestadius, L., Leavitt, S.
577 M., Minnemeyer, S., Polasky, S., Potapov, P., Putz, F. E., Sanderman, J., Silvius, M., Wollenberg, E., and
578 Fargione, J.: Natural climate solutions, *PNAS*, 114, 11645–11650, <https://doi.org/10.1073/pnas.1710465114>,
579 2017.
- 580 Gyssels, G., Poesen, J., Bochet, E., and Li, Y.: Impact of plant roots on the resistance of soils to erosion by
581 water: a review, 29, 189–217, <https://doi.org/10.1191/0309133305pp443ra>, 2005.
- 582 Harris, I., Osborn, T. J., Jones, P., and Lister, D.: Version 4 of the CRU TS monthly high-resolution gridded
583 multivariate climate dataset, 7, 109, <https://doi.org/10.1038/s41597-020-0453-3>, 2020.
- 584 Heijden, M. G. A. V. D., Bardgett, R. D., and Straalen, N. M. V.: The unseen majority: soil microbes as drivers
585 of plant diversity and productivity in terrestrial ecosystems, 11, 296–310, <https://doi.org/10.1111/j.1461-0248.2007.01139.x>, 2008.
- 587 Hempel, S., Frieler, K., Warszawski, L., Schewe, J., and Piontek, F.: Bias corrected GCM input data for ISIMIP
588 Fast Track, <https://doi.org/10.5880/PIK.2016.001>, 2013.
- 589 Herzfeld, T., Müller, C., Heinke, J., Rolinski, S., and Porwollik, V.: LPJmL Model Source Code (version 5.0-
590 tillage2). <https://doi.org/10.5281/zenodo.4625868>, 2021.
- 591 Hiederer, R., Köchy, M., European Commission, Joint Research Centre, and Institute for Environment and
592 Sustainability: Global soil organic carbon estimates and the harmonized world soil database., Publications
593 Office, Luxembourg, 2011.
- 594 Hurtt, G. C., Chini, L., Sahajpal, R., Frohling, S., Bodirsky, B. L., Calvin, K., Doelman, J. C., Fisk, J., Fujimori,
595 S., Goldewijk, K. K., Hasegawa, T., Havlik, P., Heinemann, A., Humpenöder, F., Jungclaus, J., Kaplan, J.,
596 Kennedy, J., Kristzin, T., Lawrence, D., Lawrence, P., Ma, L., Mertz, O., Pongratz, J., Popp, A., Poulter, B.,
597 Riahi, K., Shevliakova, E., Stehfest, E., Thornton, P., Tubiello, F. N., Vuuren, D. P. van, and Zhang, X.:
598 Harmonization of Global Land-Use Change and Management for the Period 850-2100 (LUH2) for CMIP6, 1–
599 65, <https://doi.org/10.5194/gmd-2019-360>, 2020.
- 600 IPCC: IPCC - Guidelines for National Greenhouse Gas Inventories, Cambridge University Press, UK, 2006.
- 601 IPCC Guidelines for National Greenhouse Gas Inventories Volume 4: Agriculture, Forestry and other Land Use.:
602 <https://www.ipcc-nggip.iges.or.jp/public/2006gl/vol4.html>.
- 603 IPCC: 2019 Refinement to the 2006 IPCC Guidelines for National Greenhouse Gas Inventories - Chapter 5 -
604 Cropland, IPCC, 2019.
- 605 Jobbágy, E. G. and Jackson, R. B.: The Vertical Distribution of Soil Organic Carbon and Its Relation to Climate
606 and Vegetation, 10, 423–436, [https://doi.org/10.1890/1051-0761\(2000\)010\[0423:TVDOSO\]2.0.CO;2](https://doi.org/10.1890/1051-0761(2000)010[0423:TVDOSO]2.0.CO;2), 2000.
- 607 Karstens, K., Bodirsky, B. L., Dietrich, J. P., Dondini, M., Heinke, J., Kuhnert, M., Müller, C., Rolinski, S.,
608 Smith, P., Weindl, I., Lotze-Campen, H., and Popp, A.: Management induced changes of soil organic carbon on
609 global croplands [preprint], in review, 1–30, <https://doi.org/10.5194/bg-2020-468>, 2020.



- 610 Kurothe, R. S., Kumar, G., Singh, R., Singh, H. B., Tiwari, S. P., Vishwakarma, A. K., Sena, D. R., and Pande,
611 V. C.: Effect of tillage and cropping systems on runoff, soil loss and crop yields under semiarid rainfed
612 agriculture in India, *Soil and Tillage Research*, 140, 126–134, <https://doi.org/10.1016/j.still.2014.03.005>, 2014.
- 613 Lal, R.: World cropland soils as a source or sink for atmospheric carbon, in: *Advances in Agronomy*, vol. 71,
614 Elsevier, 145–191, [https://doi.org/10.1016/S0065-2113\(01\)71014-0](https://doi.org/10.1016/S0065-2113(01)71014-0), 2001.
- 615 Lal, R.: Offsetting global CO₂ emissions by restoration of degraded soils and intensification of world agriculture
616 and forestry, 14, 309–322, <https://doi.org/10.1002/ldr.562>, 2003.
- 617 Lal, R.: Soil Carbon Sequestration Impacts on Global Climate Change and Food Security, 304, 1623–1627,
618 <https://doi.org/10.1126/science.1097396>, 2004.
- 619 Lal, R.: Challenges and opportunities in soil organic matter research, 60, 158–169,
620 <https://doi.org/10.1111/j.1365-2389.2008.01114.x>, 2009.
- 621 Le Quéré, C., Moriarty, R., Andrew, R. M., Canadell, J. G., Sitth, S., Korsbakken, J. I., Friedlingstein, P., Peters,
622 G. P., Andres, R. J., Boden, T. A., Houghton, R. A., House, J. I., Keeling, R. F., Tans, P., Arneeth, A., Bakker, D.
623 C. E., Barbero, L., Bopp, L., Chang, J., Chevallier, F., Chini, L. P., Ciais, P., Fader, M., Feely, R. A., Gkritzalis,
624 T., Harris, I., Hauck, J., Ilyina, T., Jain, A. K., Kato, E., Kitidis, V., Klein Goldewijk, K., Koven, C.,
625 Landschützer, P., Lauvset, S. K., Lefèvre, N., Lenton, A., Lima, I. D., Metzl, N., Millero, F., Munro, D. R.,
626 Murata, A., Nabel, J. E. M. S., Nakaoka, S., Nojiri, Y., O'Brien, K., Olsen, A., Ono, T., Pérez, F. F., Pfeil, B.,
627 Pierrot, D., Poulter, B., Rehder, G., Rödenbeck, C., Saito, S., Schuster, U., Schwinger, J., Séférian, R., Steinhoff,
628 T., Stocker, B. D., Sutton, A. J., Takahashi, T., Tilbrook, B., van der Laan-Luijkx, I. T., van der Werf, G. R., van
629 Heuven, S., Vandemark, D., Viovy, N., Wiltshire, A., Zaehle, S., and Zeng, N.: Global Carbon Budget 2015, 7,
630 349–396, <https://doi.org/10.5194/essd-7-349-2015>, 2015.
- 631 Le Quéré, C. L., Andrew, R. M., Friedlingstein, P., Sitth, S., Hauck, J., Pongratz, J., Pickers, P. A., Korsbakken,
632 J. I., Peters, G. P., Canadell, J. G., Arneeth, A., Arora, V. K., Barbero, L., Bastos, A., Bopp, L., Chevallier, F.,
633 Chini, L. P., Ciais, P., Doney, S. C., Gkritzalis, T., Goll, D. S., Harris, I., Haverd, V., Hoffman, F. M., Hoppema,
634 M., Houghton, R. A., Hurtt, G., Ilyina, T., Jain, A. K., Johannessen, T., Jones, C. D., Kato, E., Keeling, R. F.,
635 Goldewijk, K. K., Landschützer, P., Lefèvre, N., Lienert, S., Liu, Z., Lombardozi, D., Metzl, N., Munro, D. R.,
636 Nabel, J. E. M. S., Nakaoka, S., Neill, C., Olsen, A., Ono, T., Patra, P., Peregon, A., Peters, W., Peylin, P., Pfeil,
637 B., Pierrot, D., Poulter, B., Rehder, G., Resplandy, L., Robertson, E., Rocher, M., Rödenbeck, C., Schuster, U.,
638 Schwinger, J., Séférian, R., Skjelvan, I., Steinhoff, T., Sutton, A., Tans, P. P., Tian, H., Tilbrook, B., Tubiello, F.
639 N., Laan-Luijkx, I. T. van der, Werf, G. R. van der, Viovy, N., Walker, A. P., Wiltshire, A. J., Wright, R.,
640 Zaehle, S., and Zheng, B.: Global Carbon Budget 2018, 10, 2141–2194, <https://doi.org/10.5194/essd-10-2141-2018>, 2018.
- 642 Lorenz, K. and Lal, R.: Soil organic carbon sequestration in agroforestry systems. A review, *Agron. Sustain.*
643 *Dev.*, 34, 443–454, <https://doi.org/10.1007/s13593-014-0212-y>, 2014.
- 644 Luo, Y., Ahlström, A., Allison, S. D., Batjes, N. H., Brovkin, V., Carvalhais, N., Chappell, A., Ciais, P.,
645 Davidson, E. A., Finzi, A., Georgiou, K., Guenet, B., Hararuk, O., Harden, J. W., He, Y., Hopkins, F., Jiang, L.,
646 Koven, C., Jackson, R. B., Jones, C. D., Lara, M. J., Liang, J., McGuire, A. D., Parton, W., Peng, C., Randerson,
647 J. T., Salazar, A., Sierra, C. A., Smith, M. J., Tian, H., Todd-Brown, K. E. O., Torn, M., Groenigen, K. J. van,
648 Wang, Y. P., West, T. O., Wei, Y., Wieder, W. R., Xia, J., Xu, X., Xu, X., and Zhou, T.: Toward more realistic
649 projections of soil carbon dynamics by Earth system models, 30, 40–56, <https://doi.org/10.1002/2015GB005239>,
650 2016.
- 651 Luo, Z., Wang, E., and Sun, O. J.: Can no-tillage stimulate carbon sequestration in agricultural soils? A meta-
652 analysis of paired experiments, 139, 224–231, <https://doi.org/10.1016/j.agee.2010.08.006>, 2010.
- 653 Lutz, F., Stoorvogel, J. J., and Müller, C.: Options to model the effects of tillage on N₂O emissions at the global
654 scale, *Ecological Modelling*, 392, 212–225, <https://doi.org/10.1016/j.ecolmodel.2018.11.015>, 2019a.



- 655 Lutz, F., Herzfeld, T., Heinke, J., Rolinski, S., Schaphoff, S., Bloh, W. von, Stoorvogel, J. J., and Müller, C.:
656 Simulating the effect of tillage practices with the global ecosystem model LPJmL (version 5.0-tillage), 12, 2419–
657 2440, <https://doi.org/10.5194/gmd-12-2419-2019>, 2019b.
- 658 Macdonald, C. A., Delgado-Baquerizo, M., Reay, D. S., Hicks, L. C., and Singh, B. K.: Soil Nutrients and Soil
659 Carbon Storage, in: *Soil Carbon Storage*, Elsevier, 167–205, [https://doi.org/10.1016/B978-0-12-812766-](https://doi.org/10.1016/B978-0-12-812766-7.00006-8)
660 7.00006-8, 2018.
- 661 Mekki, A., Aloui, F., and Sayadi, S.: Influence of biowaste compost amendment on soil organic carbon storage
662 under arid climate, 69, 867–877, <https://doi.org/10.1080/10962247.2017.1374311>, 2019.
- 663 Minasny, B., Malone, B. P., McBratney, A. B., Angers, D. A., Arrouays, D., Chambers, A., Chaplot, V., Chen,
664 Z.-S., Cheng, K., Das, B. S., Field, D. J., Gimona, A., Hedley, C. B., Hong, S. Y., Mandal, B., Marchant, B. P.,
665 Martin, M., McConkey, B. G., Mulder, V. L., O'Rourke, S., Richer-de-Forges, A. C., Odeh, I., Padarian, J.,
666 Paustian, K., Pan, G., Poggio, L., Savin, I., Stolbovov, V., Stockmann, U., Sulaeman, Y., Tsui, C.-C., Vågen, T.-
667 G., van Wesemael, B., and Winowiecki, L.: Soil carbon 4 per mille, *Geoderma*, 292, 59–86,
668 <https://doi.org/10.1016/j.geoderma.2017.01.002>, 2017.
- 669 Minoli, S., Müller, C., Elliott, J., Ruane, A. C., Jägermeyr, J., Zabel, F., Dury, M., Folberth, C., François, L.,
670 Hank, T., Jacquemin, I., Liu, W., Olin, S., and Pugh, T. A. M.: Global Response Patterns of Major Rainfed
671 Crops to Adaptation by Maintaining Current Growing Periods and Irrigation, 7, 1464–1480,
672 <https://doi.org/10.1029/2018EF001130>, 2019.
- 673 Minx, J. C., Lamb, W. F., Callaghan, M. W., Fuss, S., Hilaire, J., Creutzig, F., Amann, T., Beringer, T., Garcia,
674 W. de O., Hartmann, J., Khanna, T., Lenzi, D., Luderer, G., Nemet, G. F., Rogelj, J., Smith, P., Vicente, J. L. V.,
675 Wilcox, J., and Dominguez, M. del M. Z.: Negative emissions—Part 1: Research landscape and synthesis,
676 *Environ. Res. Lett.*, 13, 063001, <https://doi.org/10.1088/1748-9326/aabf9b>, 2018.
- 677 Naipal, V., Ciais, P., Wang, Y., Lauerwald, R., Guenet, B., and Oost, K. V.: Global soil organic carbon removal
678 by water erosion under climate change and land use change during AD 1850–2005, 15, 4459–4480,
679 <https://doi.org/10.5194/bg-15-4459-2018>, 2018.
- 680 Nishina, K., Ito, A., Beerling, D. J., Cadule, P., Ciais, P., Clark, D. B., Falloon, P., Friend, A. D., Kahana, R.,
681 Kato, E., Keribin, R., Lucht, W., Lomas, M., Rademacher, T. T., Pavlick, R., Schaphoff, S., Vuichard, N.,
682 Warszawski, L., and Yokohata, T.: Quantifying uncertainties in soil carbon responses to changes in global
683 mean temperature and precipitation, *Earth Syst. Dynam.*, 5, 197–209, <https://doi.org/10.5194/esd-5-197-2014>,
684 2014.
- 685 Olin, S., Lindeskog, M., Pugh, T. a. M., Schurgers, G., Wärlind, D., Mishurov, M., Zaehle, S., Stocker, B. D.,
686 Smith, B., and Arneth, A.: Soil carbon management in large-scale Earth system modelling: implications for crop
687 yields and nitrogen leaching, 6, 745–768, <https://doi.org/10.5194/esd-6-745-2015>, 2015.
- 688 Pan, G., Smith, P., and Pan, W.: The role of soil organic matter in maintaining the productivity and yield stability
689 of cereals in China, *Agr Ecosyst Environ*, 129, 344–348, <https://doi.org/10.1016/j.agee.2008.10.008>, 2009.
- 690 Pingali, P. L.: Green Revolution: Impacts, limits, and the path ahead, *PNAS*, 109, 12302–12308,
691 <https://doi.org/10.1073/pnas.0912953109>, 2012.
- 692 Porwollik, V., Rolinski, S., Heinke, J., and Müller, C.: Generating a rule-based global gridded tillage dataset, 11,
693 823–843, <https://doi.org/10.5194/essd-11-823-2019>, 2019.
- 694 Powlson, D. S., Stirling, C. M., Jat, M. L., Gerard, B. G., Palm, C. A., Sanchez, P. A., and Cassman, K. G.:
695 Limited potential of no-till agriculture for climate change mitigation, 4, 678–683,
696 <https://doi.org/10.1038/nclimate2292>, 2014.



- 697 Pugh, T. A. M., Arneeth, A., Olin, S., Ahlström, A., Bayer, A. D., Klein Goldewijk, K., Lindeskog, M., and
698 Schurgers, G.: Simulated carbon emissions from land-use change are substantially enhanced by accounting for
699 agricultural management, 10, 124008, <https://doi.org/10.1088/1748-9326/10/12/124008>, 2015.
- 700 Ray, D. K., Ramankutty, N., Mueller, N. D., West, P. C., and Foley, J. A.: Recent patterns of crop yield growth
701 and stagnation, *Nat Commun*, 3, 1–7, <https://doi.org/10.1038/ncomms2296>, 2012.
- 702 Ren, W., Banger, K., Tao, B., Yang, J., Huang, Y., and Tian, H.: Global pattern and change of cropland soil
703 organic carbon during 1901–2010: Roles of climate, atmospheric chemistry, land use and management,
704 *Geography and Sustainability*, 1, 59–69, <https://doi.org/10.1016/j.geosus.2020.03.001>, 2020.
- 705 Rogelj, J., den Elzen, M., Höhne, N., Fransen, T., Fekete, H., Winkler, H., Schaeffer, R., Sha, F., Riahi, K., and
706 Meinshausen, M.: Paris Agreement climate proposals need a boost to keep warming well below 2 °C, 534, 631–
707 639, <https://doi.org/10.1038/nature18307>, 2016.
- 708 Rogelj, J., Popp, A., Calvin, K. V., Luderer, G., Emmerling, J., Gernaat, D., Fujimori, S., Strefler, J., Hasegawa,
709 T., Marangoni, G., Krey, V., Kriegler, E., Riahi, K., van Vuuren, D. P., Doelman, J., Drouet, L., Edmonds, J.,
710 Fricko, O., Harmsen, M., Havlik, P., Humpenöder, F., Stehfest, E., and Tavoni, M.: Scenarios towards limiting
711 global mean temperature increase below 1.5 °C. *Nature Climate Change* 8 (4): 325–332.,
712 <https://doi.org/10.1038/s41558-018-0091-3>, 2018.
- 713 Sanderman, J., Hengl, T., and Fiske, G. J.: Soil carbon debt of 12,000 years of human land use, *PNAS*, 114,
714 9575–9580, <https://doi.org/10.1073/pnas.1706103114>, 2017.
- 715 Schaphoff, S., Heyder, U., Ostberg, S., Gerten, D., Heinke, J., and Lucht, W.: Contribution of permafrost soils to
716 the global carbon budget, 8, 014026, <https://doi.org/10.1088/1748-9326/8/1/014026>, 2013.
- 717 Schaphoff, S., Bloh, W. von, Rammig, A., Thonicke, K., Biemans, H., Forkel, M., Gerten, D., Heinke, J.,
718 Jägermeyr, J., Knauer, J., Langerwisch, F., Lucht, W., Müller, C., Rolinski, S., and Waha, K.: LPJmL4 – a
719 dynamic global vegetation model with managed land – Part 1: Model description, 11, 1343–1375,
720 <https://doi.org/10.5194/gmd-11-1343-2018>.
- 721 Scharlemann, J. P., Tanner, E. V., Hiederer, R., and Kapos, V.: Global soil carbon: understanding and managing
722 the largest terrestrial carbon pool, 5, 81–91, <https://doi.org/10.4155/cmt.13.77>, 2014.
- 723 Sitch, S., Smith, B., Prentice, I. C., Arneeth, A., Bondeau, A., Cramer, W., Kaplan, J. O., Levis, S., Lucht, W.,
724 Sykes, M. T., and others: Evaluation of ecosystem dynamics, plant geography and terrestrial carbon cycling in
725 the LPJ dynamic global vegetation model, 9, 161–185, 2003.
- 726 Smith, P.: Soil carbon sequestration and biochar as negative emission technologies, *Glob Change Biol*, 22, 1315–
727 1324, <https://doi.org/10.1111/gcb.13178>, 2016.
- 728 Stehfest, E., van Zeist, W.-J., Valin, H., Havlik, P., Popp, A., Kyle, P., Tabeau, A., Mason-D’Croz, D.,
729 Hasegawa, T., Bodirsky, B. L., Calvin, K., Doelman, J. C., Fujimori, S., Humpenöder, F., Lotze-Campen, H.,
730 van Meijl, H., and Wiebe, K.: Key determinants of global land-use projections, 10, 2166,
731 <https://doi.org/10.1038/s41467-019-09945-w>, 2019.
- 732 Stella, T., Mouratiadou, I., Gaiser, T., Berg-Mohnicke, M., Wallor, E., Ewert, F., and Nendel, C.: Estimating the
733 contribution of crop residues to soil organic carbon conservation, *Environ. Res. Lett.*, 14, 094008,
734 <https://doi.org/10.1088/1748-9326/ab395c>, 2019.
- 735 Stockmann, U., Adams, M. A., Crawford, J. W., Field, D. J., Henakaarchchi, N., Jenkins, M., Minasny, B.,
736 Mcbratney, A. B., Courcelles, V. D. R. D., Singh, K., Wheeler, I., Abbott, L., Angers, D. A., Baldock, J., Bird,
737 M., Brookes, P. C., Chenu, C., Jastrow, J. D., Lal, R., Lehmann, J., O’Donnell, A. G., Parton, W. J., Whitehead,



- 738 D., and Zimmermann, M.: The knowns, known unknowns and unknowns of sequestration of soil organic carbon,
739 164, 80–99, <https://doi.org/10.1016/j.agee.2012.10.001>, 2013.
- 740 Subira, J., Ammar, K., Álvaro, F., García del Moral, L. F., Dreisigacker, S., and Royo, C.: Changes in durum
741 wheat root and aerial biomass caused by the introduction of the Rht-B1b dwarfing allele and their effects on
742 yield formation, *Plant Soil*, 403, 291–304, <https://doi.org/10.1007/s11104-015-2781-1>, 2016.
- 743 ESRL Global Monitoring Division - Global Greenhouse Gas Reference Network:
744 <https://www.esrl.noaa.gov/gmd/ccgg/trends/>, last access: 12 July 2018.
- 745 Torres, A. B., Marchant, R., Lovett, J. C., Smart, J. C. R., and Tipper, R.: Analysis of the carbon sequestration
746 costs of afforestation and reforestation agroforestry practices and the use of cost curves to evaluate their potential
747 for implementation of climate change mitigation, *ECOL ECON*, 69, 469–477,
748 <https://doi.org/10.1016/j.ecolecon.2009.09.007>, 2010.
- 749 United Nations, Department of Economic and Social Affairs, and Population Division: World population
750 prospects Highlights, 2019 revision Highlights, 2019 revision, 2019.
- 751 de Vries, W.: Soil carbon 4 per mille: a good initiative but let's manage not only the soil but also the
752 expectations, 309, 111–112, <https://doi.org/10.1016/j.geoderma.2017.05.023>, 2018.
- 753 White, R. E., Davidson, B., Lam, S. K., and Chen, D.: A critique of the paper 'Soil carbon 4 per mille' by
754 Minasny et al. (2017), 309, 115–117, <https://doi.org/10.1016/j.geoderma.2017.05.025>, 2018.
- 755 Wik, M., Pingali, P., and Broca, S.: Global Agricultural Performance: Past Trends and Future Prospects, World
756 Development Report 2008, 39, 2008.
- 757 Zhang, B., Tian, H., Lu, C., Dangal, S. R. S., Yang, J., and Pan, S.: Global manure nitrogen production and
758 application in cropland during 1860–2014: a 5 arcmin gridded global dataset for Earth system modeling, 9, 667–
759 678, <https://doi.org/10.5194/essd-9-667-2017>, 2017.
- 760 Zomer, R. J., Bossio, D. A., Sommer, R., and Verchot, L. V.: Global Sequestration Potential of Increased
761 Organic Carbon in Cropland Soils, 7, 15554, <https://doi.org/10.1038/s41598-017-15794-8>, 2017.
- 762